새로운 화재용 스프링 클러 해드의 CAE 기반 분석용 간편 방법
Simplified Approach for the CAE-based Analysis of a Novel Fire Sprinkler Head

*정태진[1], 헨리 팡가니반[1], 오주환[2]
*#T. J. Chung(tjchung@kunsan.ac.kr)[1], H. Panganiban[1] , J. H.Oh[2]
[1] 군산대학교 기계공학과, [2]마스테코

Key words : Fire sprinkler head, CAE-based analysis

1. Introduction

The use of CAE simulations has expanded fast since high speed computers are becoming affordable. Industrial companies regardless of size can now evaluate designs and improve products economically and efficiently. In academia, the usefulness is unquestionable.

In this work, we analyze a novel sprinkler head assembly. Due to the physical size of its components and the complexity of the assembly as whole, analytical approach is tedious. Likewise experimental procedure requires special measuring and data acquisition devices. In this article we present a method to solve a practical problem in which CAE simulation program is the major tool along with simple scientific approach. ANSYS Workbench [1] is used in the simulation.

2. Problem description

Shown in Fig. 1 is the sprinkler head assembly. Considering static equilibrium condition, among others we sought to determine the normal stress on the fuse metal.

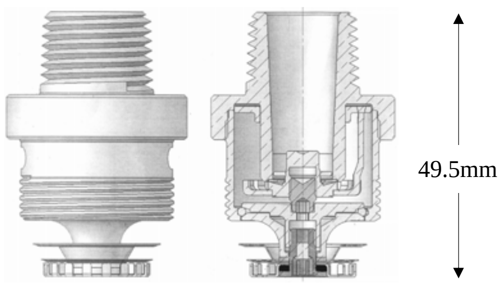

Fig. 1 Sprinkler head: side and section view

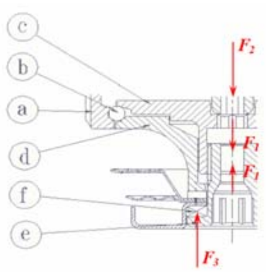

ⓐ	Frame
ⓑ	Retainer ring
ⓒ	Inner loading plate
ⓓ	Outer loading plate
ⓔ	Setting screw
ⓕ	Fuse metal
F_1	Tightening load
F_2	Force exerted due to the turning of in-place screw (not shown)
F_3	Force acting on the fuse metal due the application of the load F_1 and F_2

Fig. 2 Sprinkler head parts and loading condition

Essentially, the sprinkler parts are assembled in two steps. Referring to Fig. 2, in step 1, the inner loading plate, retainer ring, outer loading plate and fuse metal are held together by tightening the locking screw. In effect the retainer ring stretches until it sets into the slot in the frame. Step 2 is done by turning the in-place screw (not shown) pushing the bottom of the inner loading plate to the direction indicated by F2 and causing the retainer ring to slightly deform inwards fitting the whole assembly. It is known that due to the tightening of the locking screw (100 kgf-mm torque), the resulting tightening axial force is F1 = 100kgf (981N) and F2 = 60kgf (588.6N). This scenario brings out the intuition that the reverse action of the retainer ring relieves the strain energy absorbed by the fuse metal. In particular we are interested of quantifying the stress distribution within the fuse metal.

3. Analysis and simulation

The actual assembly has several parts resulting to many contact surfaces. Contact surfaces require nonlinear analysis and often difficult to model and obtain convergence of FEA solution. However in this problem, since we are interested only with the normal stress in the fuse metal we can build an ideal model neglecting the effect of contacting areas of insignificant contribution to the normal stress and focus only on areas essential to the analysis. In this case, load transfer physics occurring within the interaction of the outer loading plate, retainer ring, inner loading plates and the frame can be assumed negligible compared to the applied forces F1 and F2. One can easily justify such assumption by the fact that even if we apply F2 directly opposite to the action of F1 the effect is theoretically “nothing”. Nonetheless, the stiffness or damping effect created by such interaction should be properly accounted for. Thus we can build a model where a lumped stiffness representing the interaction of the mentioned components is used as shown in Fig. 3.

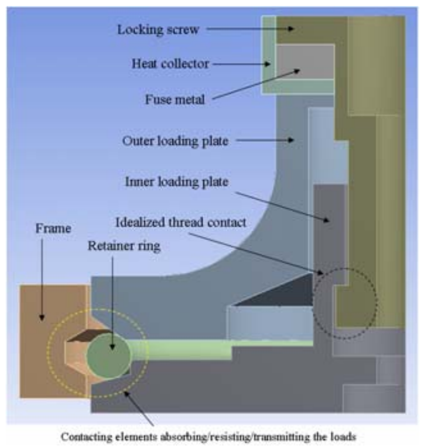

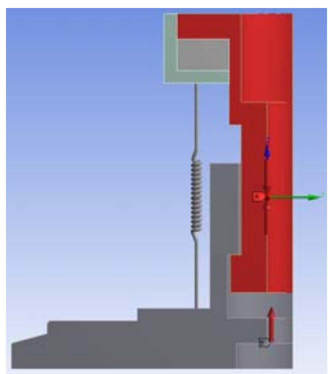

Fig. 3 Idealized model of the sprinkler head. Top: cut-away view, bottom: section view.

When the locking screw is tightened up to 100kgf-mm torque (100kgf axial), this tightening force is resisted by the friction forces on the contact surfaces and absorbed by the elastic property of the contacting elements indicated in Fig. 3 (top). As been pointed out, the effect of the indicated contacting elements is negligible. However these elements or parts serve as support to the applied tightening force produced by the locking screw. In order to avoid the complexity of the contacting elements in supporting or transmitting the locking screw tightening load, these elements are removed and replaced by a spring functioning as the same. The tension/compression spring is attached to the bottom surface of the heat collector and to another surface on the inner loading plate positioned vertically. Fig. 3 (bottom) illustrates how the locking screw tightening load F1 (label A) and second load, F2 (Label B) are imposed.

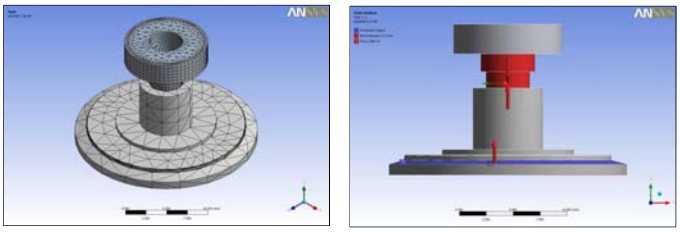

Fig. 4. Mesh and boundary condition

The full model used in the simulation is shown in Fig. 4. Note that a reasonable fine mesh Fig. 4(left) is defined at contacting areas. Fig. 4(right) shows the imposed boundary conditions and applied load. The locking screw tightening load is applied as bolt pretension. Since the bolt pretension load is 100kgf the pre-adjustment length is 0.73mm, the bolt pretension can be applied in two ways – as a load or as pre-adjustment length. Here we choose as pre-adjustment length for convenience based on the experience during simulation. For the spring to correctly represent the lumped stiffness of the removed contacting elements, with the given pre-adjustment length we assumed that the reaction force underneath the locking screw head should be 100kgf (981N). It means that a suitable stiffness constant has to be specified. The suitable stiffness constant is known by first assuming a linear relation between the load and adjustment length which gives k = 1.343 kN/mm.

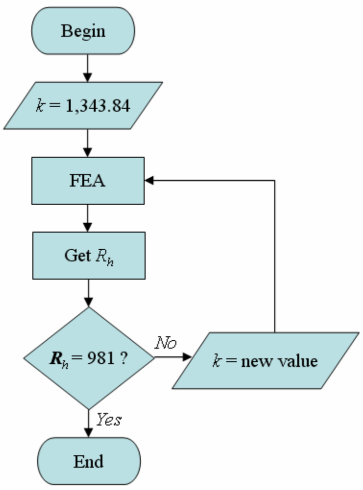

Fig.5 Lumped stiffness constant identification procedure

At the current value of the stiffness constant, check the reaction force, Rh directly underneath the screw head. The check can be conveniently carried out in ANSYS Workbench by inserting a Force Reaction Probe on the area of interest i.e. underneath the locking screw head. The reaction force must be very close to 100kgf (≈981N). If not, then change the spring constant and check the reaction force again. The whole process is repeated until the reaction force becomes 100kgf. When it does, the value is used to simulate the lumped spring stiffness constant. Note that theoretical approaches for stiffness lumping maybe employed [2,3]. Here, we used the iterative trial-and-error approach and obtained k = 1.386 kN/mm and Rh = 981.04 N. The process is depicted in Fig. 5.

4. Results and discussions

We focused our attention to the determination of the normal (compressive/tensile) stress on the fuse metal. The task was simply done by inserting a normal stress tool on the surfaces of the fuse metal. At the end of the load step the results were found as shown in the Fig. 6.

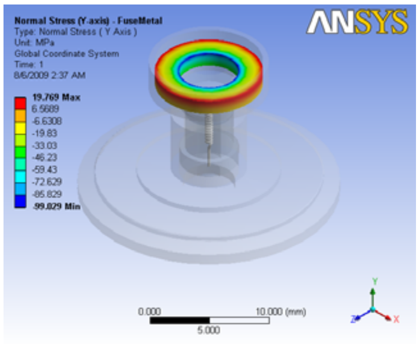

Fig. 6. Normal stress contour in the fuse metal (19.77MPa max.)

For the fuse metal, minimum and maximum stresses occurred on the top surface Fig. 6. The positive value stands for tensile and negative for compressive stress. The result showed that due to the bolt pretension the bottom surface of the locking screw head presses against the upper surface of the fuse metal. It can be observed that the stress is not uniformly compressive. Instead a varying stress that is compressive on the inner surface and slowly becomes tensile towards the outer surface. This is due to the fact that the pull of the bolt pretension is higher near the contacting surfaces between the locking screw and the fuse metal in reaction to the stiffness provided by the heat collector and the lumped spring..

Conclusions

Static analysis of the novel sprinkler head is performed using a lumped spring replacing the outer loading plate, retainer ring and the frame and neglecting the details of load transfer mechanism due to contact. Using the presented approach, simulation of complex assembly can be done more simply. On the other hand, an experimental procesure can further verify the results.

Reference

1. ANSYS® Academic Research, Release 11.0
2. Shah, S. J., "Finite-Element Geometric Stiffness Matrix Lumping By Numerical Integration For Stability Analysis", Transaction, SMiRT 16, 2001
3. Carbone, G., et.al., "Numerical and Experimental Estimation of Stiffness Performances for the Humanoid Robot WABIAN-RV", Proc. 2003 IEEE/ASME, p. 962-967